Pore cross-section area on predicting elastic properties of trabecular bovine bone for human implants

Alfredo Maciel[a],*, Gerardo Presbítero[a], Cristina Piña[a], María del Pilar Gutiérrez[b], José Guzmán[c] and Nadia Munguía[d]

[a]Instituto de Investigaciones en Materiales. Avenida Universidad 3000. Col. Universidad Nacional Autónoma de México. Delegación Coyoacán. C. P. 04510, México, D. F., México.

[b] Escuela Superior de Apan, UAEH. Carretera Apan-Calpulalpan Km 8. Chimalpa Tlalayote s/n. Col. Chimalpa, Apan, Hgo. México. C. P. 43900.
[c]CICATA-Instituto Politécnico Nacional, Col Irrigación, CP. 11500. Del. Miguel Hidalgo, México, D. F.

[d]Facultad de Química. Avenida Universidad 3000. Col. Universidad Nacional Autónoma de México. Delegación Coyoacán. C. P. 04510, México, D. F., México.

*Address for correspondence: Alfredo Maciel, Instituto de Investigaciones en Materiales. Universidad Nacional Autónoma de México. Col. Universidad Nacional Autónoma de México, Del. Coyoacán. México, D. F. México C.P. 04510. Tel. + 52 (55) 56 22 45 90, fax: + 52 (55) 56 16 12 01. E-mail: macielal@unam.mx

Abstract. A clear understanding of the dependence of mechanical properties of bone remains a task not fully achieved. In order to estimate the mechanical properties in bones for implants, pore cross-section area, calcium content, and apparent density were measured in trabecular bone samples for human implants. Samples of fresh and defatted bone tissue, extracted from one year old bovines, were cut in longitudinal and transversal orientation of the trabeculae. Pore cross-section area was measured with an image analyzer. Compression tests were conducted into rectangular prisms. Elastic modulus presents a linear tendency as a function of pore cross-section area, calcium content and apparent density regardless of the trabecular orientation. The best variable to estimate elastic modulus of trabecular bone for implants was pore cross-section area, and affirmations to consider Nukbone process appropriated for marrow extraction in trabecular bone for implantation purposes are proposed, according to bone mechanical properties. Considering stress-strain curves, defatted bone is stiffer than fresh bone. Number of pores against pore cross section area present an exponential decay, consistent for all the samples. These graphs also are useful to predict elastic properties of trabecular samples of young bovines for implants.

Key words: Elastic modulus, bone implants, trabecular bone, bone fragility

1. **Introduction**

Bone fracture risk is the reason many researchers investigate bone structure, in order to predict a possible failure *in situ.* Another reason to study trabecular bone structure is to evaluate bone quality for implant purposes. Porosity, bone architecture and chemical composition are some of the most important factors in analyzing fracture risk. This has motivated the extensive search for new ways of measuring them. Bone tissue properties depend on many factors, such as composition, age, bone structure, mineralization, micro and nanostructures. Those factors have direct impact on the mechanical properties of trabecular bone [1-4]. Calcium is the main mineral component of bone, and 99.9% of calcium content in the body can be found in this hard tissue [5]. Furthermore, mechanical properties of bone are closely related to this element as a component of hydroxyapatite.

In previous works, linear and power law correlations are the more frequent tendencies obtained when studying relationships of elastic modulus with morphology, bone architecture and chemical composition. For elastic modulus and calcium content, a power law model fits the data better than a linear model [6]. This same author reported that, as calcium content increases, so does elastic modulus [7]. Content and quality of collagen was considered as a modifier of toughness and elastic properties of bone as well [8-11]. As a measure of bone quality, calcium content is also related to other variables like apparent density and porosity. Sophisticated techniques such as elasticity imaging (elastography), micro-computed tomography and dual energy X-ray absorptiometry (DEXA) have been used to study the mechanical properties of trabecular bone, as a function of trabecular orientation and pore structure [12-16]. Other researchers have confirmed that mechanical properties are anisotropic and also vary with trabecular thickness [17] and trabecular orientation [18]. Apparent density has been a widely used parameter to evaluate bone mechanical properties [18-25]. Apparent density has been not only an acceptable parameter to be related to mechanical properties, but also a study parameter in fracture mechanics. In most studies, power-law equations have been found to fit the data of elastic modulus against apparent density. Porosity measurements, performed with an image analyzer, were related with shear fracture toughness finding poor

correlations [26]. Until now, the way in which distribution of pores influence the mechanical properties of bones has not been precisely defined. In spite of the achievements acquired to relate bone pores with its mechanical properties, further work is necessary to find better correlations.

Fracture mechanics in linear elastic materials are described by means of two approaches: energy and stress intensity. Both approaches tell us that a crack initiates and propagates from a flaw [27]. In the case of trabecular bone, a pore could be considered a flaw that potentially can initiate a crack [28]. These authors reported a sequence of photographs taken at high speed in which, at some point, the photographs allowed them to see how trabeculae collapsed at a strain of 2.5 %. To the best of our knowledge, considering pore cross-section area as the main reason for a failure to appear, as suggested in the two theories of fracture mechanics, has not been fully considered in previous works intended to assess the risk of fracture or the mechanical properties of trabecular bone.

The aim of this work was to find out the best correlation among pore cross-section area, calcium content and apparent density with elastic modulus of trabecular bone, measuring pore cross-section area by using a simple technique, and to analyze how bone pores distribute according to their size and the elastic properties of bone. Fresh and defatted bone cut longitudinally and transversally to the trabeculae were both considered in this study.

2. Materials and methods

2.1 Sample preparation

Samples were harvested from the trabecular part of four femur condyles of one year old bovines. Four sets of 10 parallelograms of $30 \times 15 \times 15$ mm were machined. Of the four sets of samples, two sets were cut from fresh bone and the other two sets were cut from defatted bone. When cutting the samples of fresh and defatted bone, two orientations regarding the trabecular orientation were considered: longitudinal and transversal.

Special attention was given to get upper and lower surfaces of the samples plane and parallel to each other, in order for the specimens to coincide as much as possible with the surface of the compression plates of the mechanical testing machine. The defatted bone was prepared according to the Mexican patent number PA/a/2002/009719. When following the process of this patent the bone is denominated Nukbone [29]. This process includes washing out the marrow with hot water and special soaps. For fresh bone samples, the bone marrow remained in place during the compression test, in order to maintain the soft organic material in contact with the bone hard tissue, such as occurs naturally in organisms. In clinical applications, the defatted bone is to be used as implants to restore bone, while fresh bone was used only as a reference of the evolution of the properties of the bone due to the cleaning process that is applied to transform it into defatted bone. The fresh bone samples were kept frozen at -4°C until the moment of the test. After performing the compression tests, the marrow was removed following the same process used for the defatted bone samples. Photographs of the defatted bone samples were taken with a digital camera, before performing the compression tests, Pictures of fresh bone samples were taken after the compression tests and after removing the marrow. Washing out the marrow allowed us to have visible the trabeculae pores.

2.2 Pore cross-section area analysis

Pore cross-section area analysis was conducted in photographs taken in the four lateral sides of the specimens. The upper and lower sides were not considered in this analysis as they were in contact with the machine plates, and a fracture is not expected to be initiated in these sides. In this analysis, the pores considered were the visual cavities formed when the trabeculae were cut. Having painted the lateral sides in black colour for a better contrast between bone and pore cross-section areas (Figure 1), the porous structure of the trabecular bone was highly visible, allowing the correct measurement of the pore cross-section areas.

The photographs were analyzed with Image Pro Plus 3.0 software. This software

allowed us to clearly identify the pore cross-section area from the trabecular bone surface, and automatically measured the average diameter of the pores. For this, the software took at least five different diameters in a pore. The average diameter is used to calculate a pore cross-section area for each pore. The total pore cross-section area of each sample was calculated by simply adding the pore cross-section area of all the pores of the four sides.

2.3 Elastic modulus in compression

Compression tests were performed in an Instron 5500R mechanical testing machine. The speed of test was 1 mm/min. The elastic modulus was calculated as the slop in the linear part of the stress-strain curve obtained experimentally. The test was stopped after reaching the yielding point and before its catastrophic failure. Differences in the mechanical properties between fresh and defatted bovine bones in the tests performed by the current group, compared to those of human bones reported by other authors, are given in order to confirm the capability of the defatted bones to be placed as human implants, regarding their mechanical endurance.

2.4 Calcium content evaluation

Calcium content was evaluated by means of an optical emission spectroscope with inductively coupled plasma (ICP-OES). Each sample was composed of 0.1g of bone sample and 2.5ml of nitric acid, 1.5ml of perhydrol 30% (H_2O_2), and 0.3ml of hydrochloric acid. All the reagents were suprapur (Merck, Germany). This procedure was repeated once again for each sample. The samples were digested in a Parr Physica Multiwave Perkin Elmer oven. The analysis was done in an Optima 4300DV Perkin Elmer Co. USA oven with the software Parr 001H, using the solid-state detector and the high-solids nebulizer.

2.5 Apparent density measurement

Apparent density was geometrically determined in the defatted bone samples before performing the compression tests. In the case of the fresh bone samples, apparent density was determined after performing the compression tests and removing the marrow. Values were calculated from the ratio m/V, where m represents the mass of the sample and V is the geometrical total volume of the sample, including pores [30].

3. Results

3.1 Pore cross-section area and elastic modulus relationship

An examination of the elastic modulus against pore cross-section area presents a linear tendency with a negative slope for all sets of data with moderate dispersion, as shown in Figure 2(a, b). These graphs can be used to predict the elastic modulus of trabecular bone for human implants, when the pore cross-section area has been measured. Besides, this avoids applying a load that may weaken the implant material. The elastic modulus is in the range of previous works [23, 31], and the correlation factors (R^2) of the data are between 0.8 and 0.9. Elastic modulus was higher for defatted bone than for fresh bone samples: 6% in longitudinal and 23% in transversal orientation. The results are consistent with studies of denaturized bone, in which it was found that a higher mineral content contributes to increase the elastic modulus [11], and to decrease the deformation [32].

3.2 Frequencies histogram of amount of pores against pore cross-section area

The behaviour of the amount of pores against intervals of pore cross-section area in transversal samples follows an exponential and smooth decrease. A histogram of frequencies of one transversal sample is presented in Figure 3. The histogram of frequencies considers increments of 0.1 mm^2 in pore cross-section area in the x-axis

against amount of pores on the y-axis, in the same interval. This curve describes the data of the four sides with a much better R^2 (0.93) than any of the four curves of each lateral side presented in table 1, as a result of the larger amount of data considered in Figure 3.

The data of each side showed a particular distribution of pores, all of them with an exponential decline. The side with the largest pore cross-section area was chosen as number one. Side number three, being the opposite side to side one, was the second most porous side. Sides two and side four were the sides with the fewest pore cross-section area. R^2 for curves of the sides individually ranged between 0.92 and 0.85. The sum of the amount of pores, pore cross-section area, equations fitting the data and the R^2 values of pore cross-section area and number of pores of the four lateral sides and the data of Figure 3 are presented in Table 1. Although side number one has the largest pore cross-section area, side number three is the one that has the largest number of pores, being opposite to side one. The pore distribution of the four individual sides follows an exponential decrease with most of the pores smaller than, or equal to 0.5 mm^2.

3.3 Number of pores vs. pore cross-section area

A correlation between number of pores versus pore cross-section area was intended. As a result, an exponential decreasing tendency was found. All the pores in the four sides of the samples were ordered according to their areas. An increasing integer was assigned to each pore as their pore cross-section area diminished and was presented as "number of pore" in the y-axis. The behaviour was similar for fresh and defatted bone in both orientations.

The exponential equations for data with the larger and the lower elastic modulus are presented in Table 2. It is concluded, from the results, that the exponential equations for defatted bone samples have a larger R^2 (nearly 1) than the fresh bone samples (0.92), and that implies that defatted bone gives more consistent mechanical properties as a function of pore cross-section area.

3.4 Elastic modulus and calcium content

Elastic modulus showed a linear tendency with calcium content, and the higher the calcium content, the larger the elastic modulus. Their R^2 measurements were between 0.7 and 0.9, nearly 0.1 smaller than the correlation factor in the graph of elastic modulus against pore cross-section area. On the one hand, the graph corresponding to fresh bone in the transversal orientation had a slope 40% higher than its longitudinal counterpart (Figure 4(a)). On the other hand, defatted bone in the longitudinal orientation showed a slope only 6 % higher than the slope in the transversal orientation (Figure 4(b)). According to the data, elastic modulus in fresh bone samples in the transversal orientation was more sensitive to calcium content than the rest of the data sets.

3.5 Elastic modulus versus apparent density

Elastic modulus showed further a linear augmentation as the apparent density increased, and their R^2 values were presented between 0.66 and 0.8 (Figure 5 (a, b)). Apparent density values for all samples were between 0.3 and 0.9 g/cm^3, which were consistent with the studies in bovine humeri [31] and bovine tibia [20]. The slope of the graphs was higher in the transversal orientation for both fresh and defatted bone samples, as can be seen in the equations of the inset in Figure 5 (a, b). For fresh bone samples, (Figure 5 (a)), the slope was 52% higher in the transversal than in the longitudinal orientation. The elastic modulus of defatted bone in the transversal samples increases monotonically, and the slope was 17% larger than the samples cut in the longitudinal orientation (Figure 5 (b)).

3.6 Stress-strain curves in compression

Stress-strain curves of the fresh and defatted bone for both longitudinal and transversal orientations are presented in Figure 6 (a, b, c). Compressive stress was calculated at the maximum of the curve of force-displacement as force divided by the transversal area of

the sample. The strain was calculated by dividing the decrement in length of the sample divided by its original length. Pore cross-section area is indicated in the curve of each sample. Compression stress-strain curves for fresh and defatted samples in the longitudinal orientation are shown in Figure 6 (a, b); the curves showed that the maximum compressive stress (34 MPa) of defatted bone is 63% larger than the maximum compressive stress in fresh bone samples. In the same Figure 6 (a), the maximum strain (0.0264mm/mm) is, in average, nearly 10% higher for fresh bone samples than the strain for defatted bone samples. In transversal samples (Figure 6 (b, c)), the compressive stress (36 MPa) is 33% larger for the defatted bone (Figure 6 (c)) than for fresh bone (27 MPa) (Figure 6 (b)). The strain was slightly larger (≈10%) in fresh bone samples.

In general, for all sets of samples, the higher the pore cross-section area, the lower the compressive stress values. For fresh bone samples, the stress-strain curves, showed in Figure 6 (c), are separated in two groups; one group (I) with a compressive stress between 27 and 17 MPa (low porosity), and the other group(II) between 9 and 3 MPa of compressive stress (high porosity). Stress-strain curves for defatted bone samples in Figure 6 (c) are separated into one specimen (I) of high compressive stress (36 MPa) and a group of two specimens (II) between 20 and 17 MPa. At lower compressive stress, there is a group of seven specimens (III) from 10 to 3 MPa. The compressive stress decreased 1/3 from one group of curves to the other.

A comparison between the results in the current work and those reported in human bones is shown in Table 3. It contains the calculated modulus of human bones from different regions, specifying the organic integration and orientation of the trabeculae. Most of the mechanical properties reported in previous works[33-36] are lower than those determined in this work.

4. Discussion

In this study, we found that elastic modulus correlated better with pore cross-section area than with calcium content or apparent density. Regardless of their anisotropy, a linear relationship between elastic modulus and pore cross-section area was found for fresh and defatted bone in the two orientations studied. We also correlated the decreasing size of pore cross-section area, in trabecular bone samples with exponential equations.

One of the most important results in the present work is shown in Figure 2. The graphs presented can be used to predict the elastic modulus within a reasonable margin of error for fresh and defatted bone, when data of pore cross-section area being available. Ford et al. [18] calculated the elastic modulus of trabecular-tibial bones of one and two year old bovines: in longitudinal orientation being in the range of 704 - 3700 MPa, whereas in transversal orientation, the elastic modulus was found to be in the range of 306 - 1300 MPa. Regarding the tests performed and presented in the current work, the samples in the longitudinal orientation had elastic modulus values between 206 and 1600 MPa, close to those obtained by Ford et al. [18]. In the transversal orientation, our samples had values between 388 and 1590 MPa, which also coincide with the results obtained in the study of Ford. A linear tendency was found for elastic modulus as a function of calcium content and apparent density as well, although the results had a poorer correlation than the case of elastic modulus against pore cross-section area.

A linear relationship was achieved for calcium content and elastic modulus, with more similar data dispersion (130-350 mg/g) than that reported in previous works [7-8, 37], regarding calcium content [38-41]. According to the calculated correlation factors, calcium content was, after pore cross-section area, the best variable associated with elastic modulus. However, determining calcium content requires sophisticated equipment, and it is time consuming compared with measuring pore cross-section area. The effect of calcium content in the elastic modulus is clear, according to the data in Figure 4 (a, b). Calcium content showed a high effect on elastic modulus, especially in

11

defatted bone samples in the longitudinal orientation, where at 150 mg/g of calcium the modulus was 217 MPa, whereas at 340 mg/g of calcium the modulus gave a value of 1600 MPa. This same sample had a slope of 6.34, 60% larger than the slope in fresh bone samples (3.9) in the same orientation. Calcium content is the second best variable to relate with elastic modulus, after pore cross-section area.

The linear correlation of elastic modulus and apparent density in this work coincides with the study published by Keaveny and coworkers [20, 31]. However, other works [23, 25] disagree with a linear function, suggesting a power-law relationship. Failure stress and apparent density also follow a linear behavior [18], with a more similar correlation factor than that presented in the current work. Shear modulus also presents a linear behavior with apparent density [42]. Goldstein, in his literature review from 1987, noted that 14 authors found a characteristic relationship, eight of them found a linear tendency, while the other authors found a power function. As apparent density in the human femur is between 0.45 and 0.69 [25], the material produced and tested in our work has adequate apparent density to be used as an implant in humans. Elastic modulus with calcium content, and elastic modulus with apparent density, had a common tendency in fresh bone samples in transversal orientation. Elastic modulus against calcium content had a slope 40% higher in transversal orientation than the longitudinal orientation (Figure 4 (a)), while in the graph of elastic modulus against apparent density, transversal samples had a slope 52% higher than the longitudinal samples (Figure 5 (a)). Therefore, the elastic modulus in the transversal samples is much higher than in the longitudinal samples. Apparent density is the most studied variable so far; however it is the less precise option to relate with elastic modulus of the variables studied.

For fresh bone, the maximum strain to generate a crack was 2% on average, as can be seen in the stress-strain curves in the Figure 6 (a, b). Six of the samples cut in the transversal orientation were weak, and four had much higher compressive stress. The samples in the longitudinal orientation showed a systematic decrease in the compressive strength. For defatted bone samples, the strain to generate a crack varied largely. The

minimum strain for a crack to occur was 1.2%, whereas the maximum was 2.9%. Compressive strength had similar values; it decreased at higher amounts of pore cross-section area in both orientations, as can be seen in Figure 6 (a, c). The higher modulus obtained in the present results (Table 3) for defatted bone under Nukbone process, when compared with those of human bone, confirms that the bones obtained by this process are suitable to be placed as human implants.

We are aware of the limitations of this study, as we do not have information of the internal area of pores. Washing out the marrow of the fresh bone samples after testing them under compression provoked their erosion during the cleansing process of bone, and a compensation of area had to be done. Measuring the connectedness of the trabeculae and their mechanical properties may help to understand why the samples cut longitudinally regarding their trabeculae have higher compressive stress, and we suggest this as a further research goal.

More work also is needed to evaluate different-aged bones, as the ones studied here were harvested from young bovines (e.g. comparing these results with the compression properties of bovine bones between two and ten years old). However, we consider this study a major contribution to the literature because it predicts the elastic modulus not only for bone as an implant, but also in the case of bone disease, with just the information of pore cross-section area in fresh and defatted bone. It is important to remember that, although the investigation procedures used in the present work do not include exceptionally novel experimentation techniques, the results presented here integrate a very accurate method for predicting the elastic modulus of bone regarding its pore cross-section area in an affordable and efficient manner. Measuring the pore cross-section area is useful to evaluate bone quality with more accuracy than using apparent density, and it is easier to measure than evaluating calcium content.

4. Conclusions

By using an image analyzer software and digital photographs, a linear relationship was found between elastic modulus and pore cross-section area of trabecular bovine bone both fresh and defatted. The larger the pore cross-section area in the bone samples, the lower the elastic modulus. These results are useful to predict mechanical properties of bone for human implants when it is possible to have images of the trabecular bone in question. The same tendency is observed in fresh and in defatted bone, regardless of the trabecular orientation. Elastic modulus also presents a linear variation as a function of the calcium content and apparent density, although there is more data dispersion than the case of elastic modulus against pore cross-section area. Also, mechanical properties of trabecular bone samples prepared with Nukbone process are appropriated to use them as human implants.

Acknowledgements

References

[1] Follet H, Viguet-Carrin S, Burt-Pichat B, Dépalle B, Bala Y, Gineyts E, Munoz F, Arlot M, Boivin G, Chapurlat RD, Delmas PD, Bouxsein ML. Effects of preexisting microdamage, collagen cross-links, degree of mineralization, age, and architecture on compressive mechanical properties of elderly human vertebral trabecular bone. Journal of Orthopaedic Research 2011;29:481-488.

[2] Tanaka K, Tanimoto Y, Kita Y, Enoki S, Katayama T. The effects of trabecular bone

microstructure on compression property of bovine cancellous bone. Key Engineering Materials 2011; 452-453:297-300.

[3] Weiner S and Wagner HD. The material bone: Structure-mechanical function relations. Annual Review of Materials Science 1998;28:271-298.

[4] Weiner S, Traub W and Wagner D. Lamellar bone: Structure-function relations. Journal of Structural Biology 1999;126:241-255.

[5] Ferguson, N., Osteoporosis in Focus. Pharmaceutical Press, 2004.

[6] Currey JD. The effect of porosity and mineral content on the Young's modulus of elasticity of compact bone. Journal of Biomechanics 1988;21:131-139.

[7] Currey JD. Physical Characteristics affecting the tensile failure properties of compact bone. Journal of Biomechanics 1990;23:837-844.

[8] Currey JD. Role of collagen and other organics in the mechanical properties of bone. Osteoporosis Int. 2003;14:S29-S33.

[9] Zioupos P, Currey JD and Hamer AJ. The role of collagen in the declining mechanical properties of aging human cortical bone. Journal of Biomedical Materials Research 1999;45:108-116.

[10] Zysset PK. A review of morphology-elasticity relationships in human trabecular bone: theories and experiments. Journal of Biomechanics 2003;36:1469-1485.

[11] Wang S, Bank RA, TeKoppele JM, Hubbard GB, Athanasiou KA and Agrawal CM. Effect of collagen denaturation on the toughness of bone. Clinica Orthopaedics and Related Research 2000;371:228-239.

[12] Shore S.W, Barbone P E, Oberai AA, Morgan E F Transversely isotropic elasticity imaging of cancellous bone. Journal of Biomechanical Engineering 2011; 133 art. no. 061002.

[13] Wu Z-x, Lei W, Hu Y-y, Wang H-q, Wan S-y, Ma, Z-s, Sang H-x, Fu S.-c, Han Y-s. Effect of ovariectomy on BMD, micro-architecture and biomechanics of cortical and cancellous bones in a sheep model. Medical Engineering and Physics 2008;30:1112-1118.

[14] Ketcham RA and Tyan TM. Quantification and visualization of anisotropy in trabecular bone. Journal of Microscopy 2004;213:158-171.

[15] Goulet RW, Goldstein SA, Ciarelli MJ, Kuhn JL, Brown MB and Feldkamp LA. The relationship between the structural and orthogonal compressive properties of trabecular bone. Journal of Biomechanics 1994;27:375- 379.

[16] Mittra E, Rubin C and QinYX. Interrelationship of trabecular mechanical and microstructural properties in sheep trabecular bone. Journal of Biomechanics 2005;38:1229-1237.

[17] Van Lenthe GH and Huiskes R. How morphology predicts properties of trabecular structures depends on intra-specimen trabecular thickness variations. Journal of Biomechanics 2002;35:1191-1197.

[18] Ford CM and Keaveny TM. The dependence of shear failure properties of trabecular bone on apparent density and trabecular orientation. Journal of Biomechanics 1996;29:1309-1317.

[19] Goldstein SA. The mechanical properties of trabecular bone: Dependence on anatomic location and function. Journal of Biomechanics 1987;20:1055-1061.

[20] Keaveny TM, Guo XE, Watchel EF, MacMahon TA and Hayes WC. Trabecular bone exhibits fully linear elastic behavior and yields at low strains. Journal of Biomechanics 1994;27:1127-1136.

[21] Ashman RB and Rho JY. Elastic modulus of trabecular bone material. Journal of Biomechanics 1988;21:177-181.

[22] Rice JC, Cowin SC, and Bowman JA. On the dependence of the elasticity and strength of cancellous bone on apparent density. Journal of Biomechanics 1988;21:155-168.

[23] Borchers RE, Gibson LJ, Burchardt H, Hayes WC. Effect of selected thermal variables on the mechanical properties of trabecular bone. Biomaterials 1995; 16:545-551.

[24] Kang Q, An YH, Friedman RF. Mechanical properties and bone densities of canine trabecular bone. Journal of Materials Science 1998;9:263-267.

[25] Giensen EBW, Ding M, Dalstra M, Van Eijden TMGJ. Mechanical properties of cancellous bone in the human mandibular condyle are anisotropic. Journal of Biomechanics 2001;34:799-803.

[26] Yeni Y N, Norman TL. Fracture toughness of human femoral neck: effect of microstructure, composition and age. Bone 2000;26: 499-504.

[27] Anderson TL, Fracture Mechanics Fundamentals and Applications. CRC
Press. Boca Ratón. Fla. 1995.

[28] Thurner PJ, Erickson B, Scriock Z, Langan J, Scott J, Zhao M, Weaver JC, Fantner GE, Turner P, Kindt JH, Schitter G, Morse DE and Hansma P.K. High-speed photography of the development of microdamage in trabecular bone during compression. Journal of Materials Research 2006;21:1093-1100.

[29] Piña Barba MC, Procedures for the preparation of medical implants of natural hydroxyapatite. Patent request number: PA/a/2002/009719.

 [30] Cowin SC. Bone Mechanics Handbook. CRS Press. USA. 2001.

[31] Keaveny TM, Borchers RE, Gibson LJ, and Hayes WC. Trabecular bone modulus and strength can depend on specimen geometry. Journal of Biomechanics 1993; 26:991-1000.

[32] Fantner GE, Birkedal H, Kindt JH, Hassenkam T, Weaver JC, Cutroni JA, Bosma BL, Bawazer L, Finch MM, Cidade GAG, Morse DE, Stucky GD, Hansma PK. Implant of the degradation of the organic matrix on the microscopic fracture behavior of trabecular bone. Bone 2004;35:1013-1022.

 [33] Martens M, Van Audekercke R, Delport P, De Meester P and Mulier JC. The mechanical characteristics of cancellous bone at the upper femoral region. Journal of Biomechanics 1983; 16:971-983.

[34] Linde F and Sorensen HCF. The effect of different storage methods on the mechanical properties of trabecular bone. Journal of Biomechanics 1993;26:1249-1252.

[35] Majumdar S, Kothari M, Augat P, Newitt DC, Link TM, Lin, JC, Lang T, Lu Y and Genant HK. High resolution magnetic resonance imaging: three-dimensional trabecular bone architecture and biomechanical properties. Bone 1998; 22:445-454.

[36]Lindahl O. Mechanical properties of dried defatted spongy bone. Acta Orthopaedica Scandinavica 1976;47:11-19.

[37] Currey JD. What determines the bending strength of compact bone? The Journal of Experimental Biology 1999;202:2495-2503.

[38]Broulik PD, Rosenkranková J, Ruzicka P, Sedlácek R, Kurcová I. The effect of chronic nicotine administration on bone mineral content and bone strength in normal and castrated male rats. Original Clinical. 2007;39:20-24.

[39]Brzóska MM, Moniuszko-Jakoniuk J. Effect of chronic exposure to calcium on the mineral status and mechanical properties of lumbar spine of male rats. Toxicology letters 2005;157:161-172.

[40]Kobayashi M, Hara K, Akiyama Y. Effects of vitamin K_2 (menatetrenone) andalendronate on bone mineral density and bone strength in rats fed a low-magnesium diet. Bone 2004;35:1136-1143.

[41]Shiga K, Hara H, Okano G, Ito M, Minami A, Tomita F. Ingestion of difructoseanhydride III and voluntary running exercise independently increase femoral and tibial bone mineral density and bone strength with increasing calcium absoption in rats. Nutrient metabolism 2003;133:4207-4211.

[42]Bruyère-Garnier K, Dumas R, Rumerhart C, Arlot M E. Mechanical characterization in shear of human femoral cancellous bone: torsion and shear stress. Medical Engineering and Physics 1999;21:641-649.
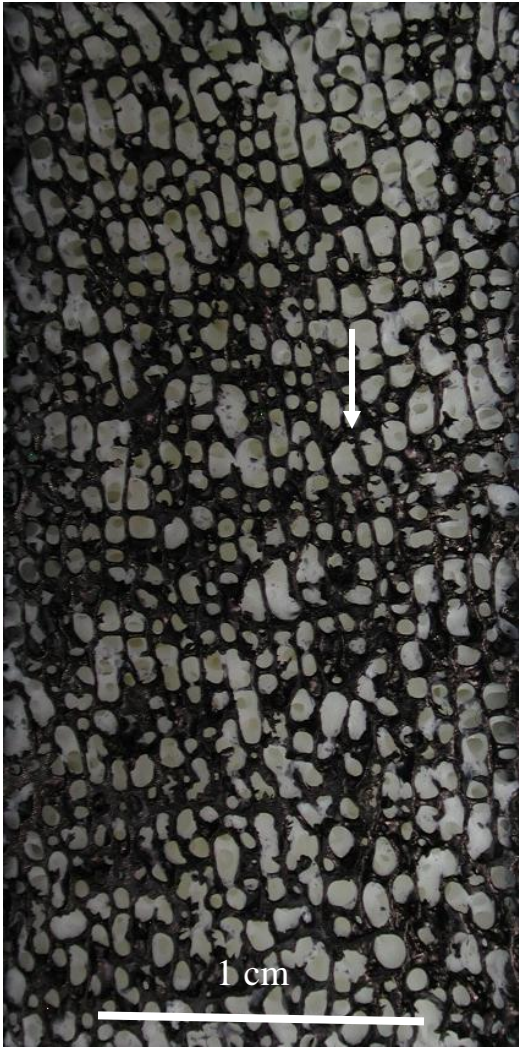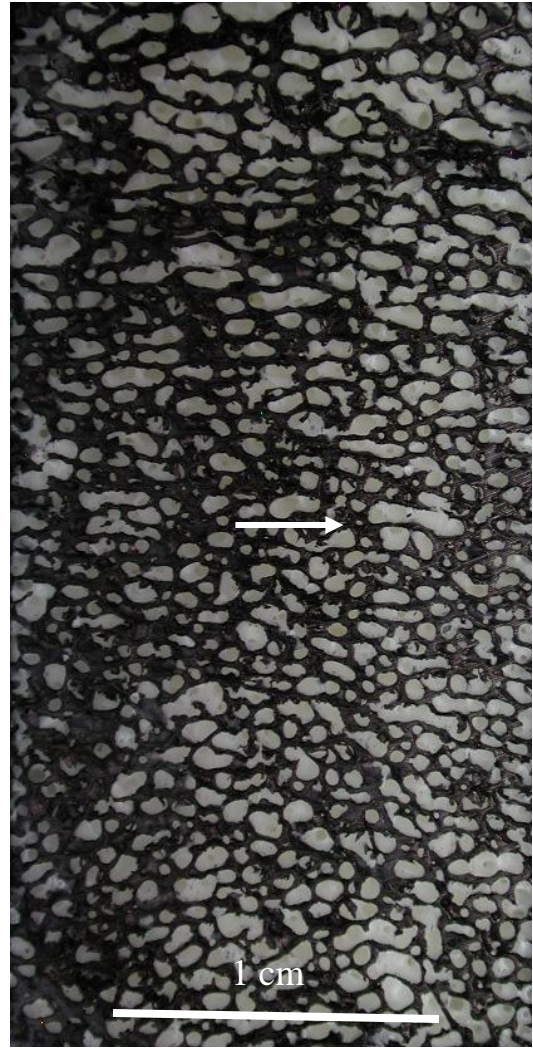
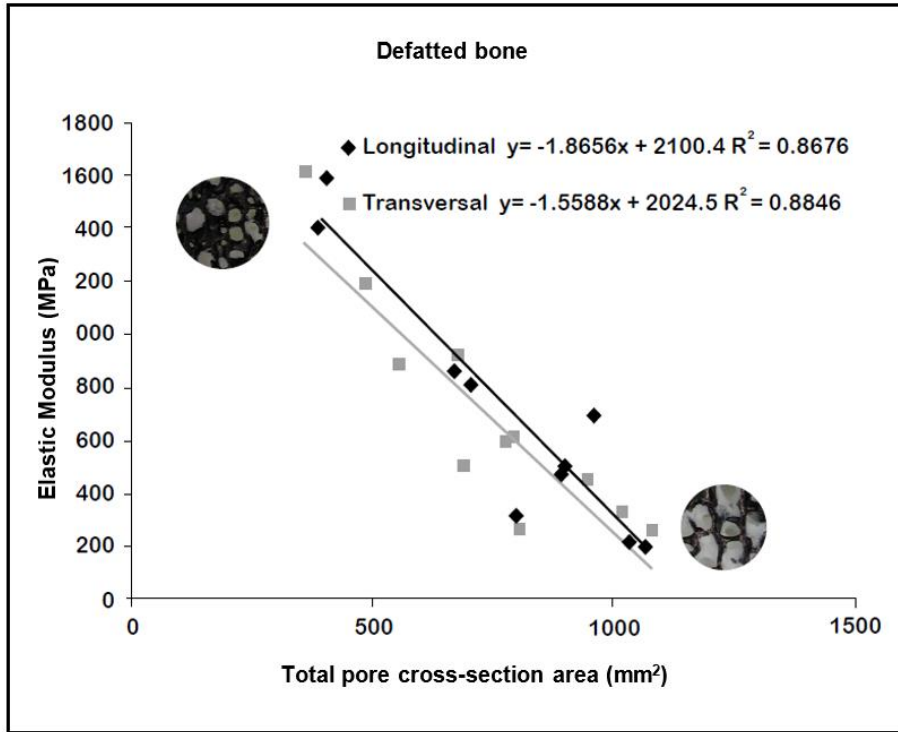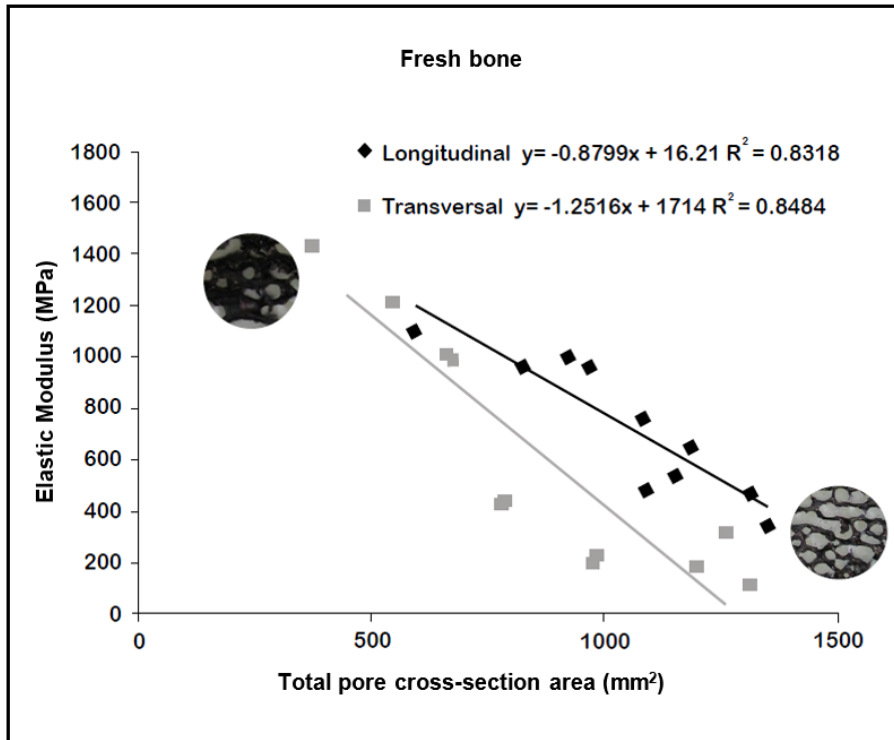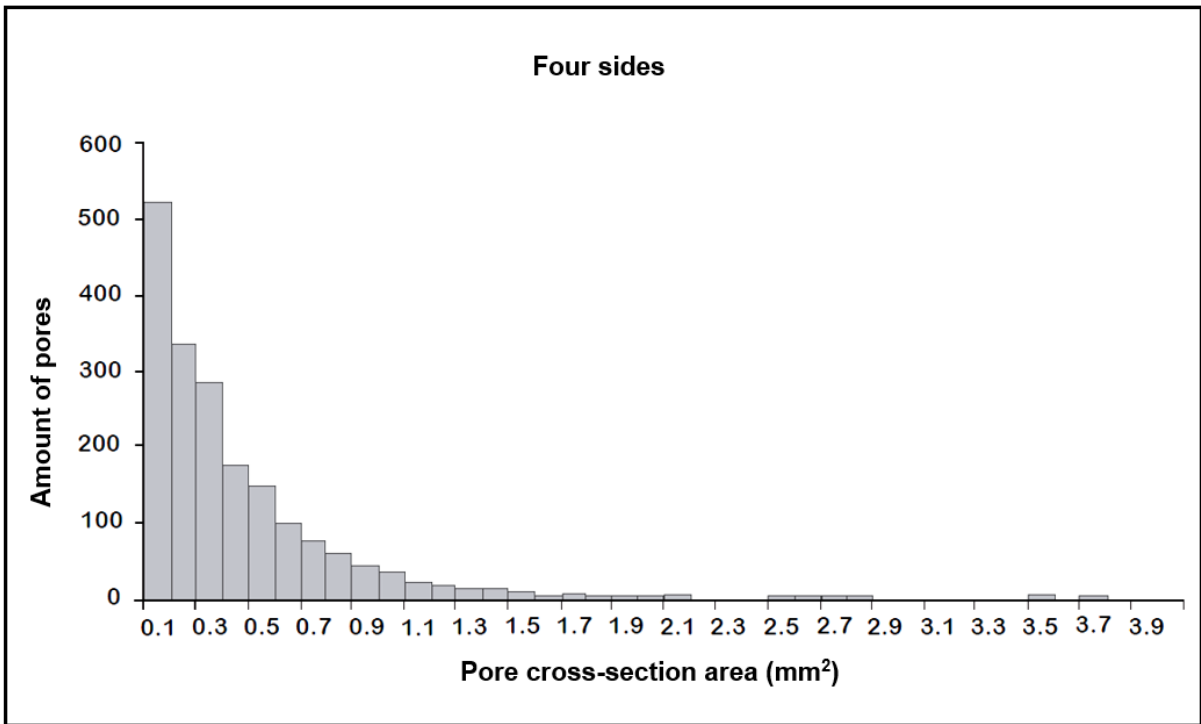(a)   (b)

Fig. 1

Fig. 2 (a)

Fig. 2 (b)

Fig. 3
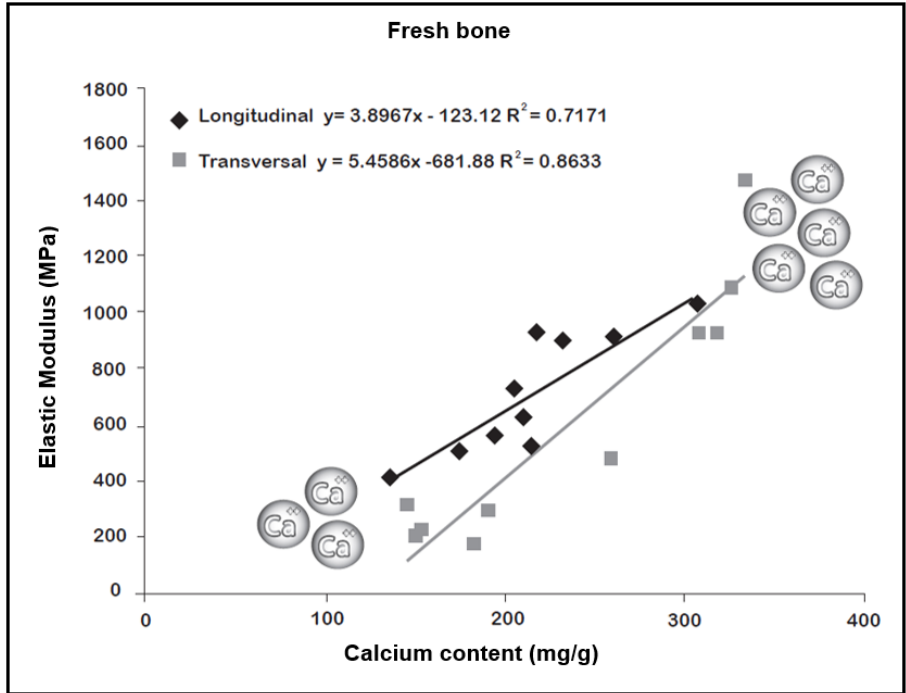
Fig. 4 (a)
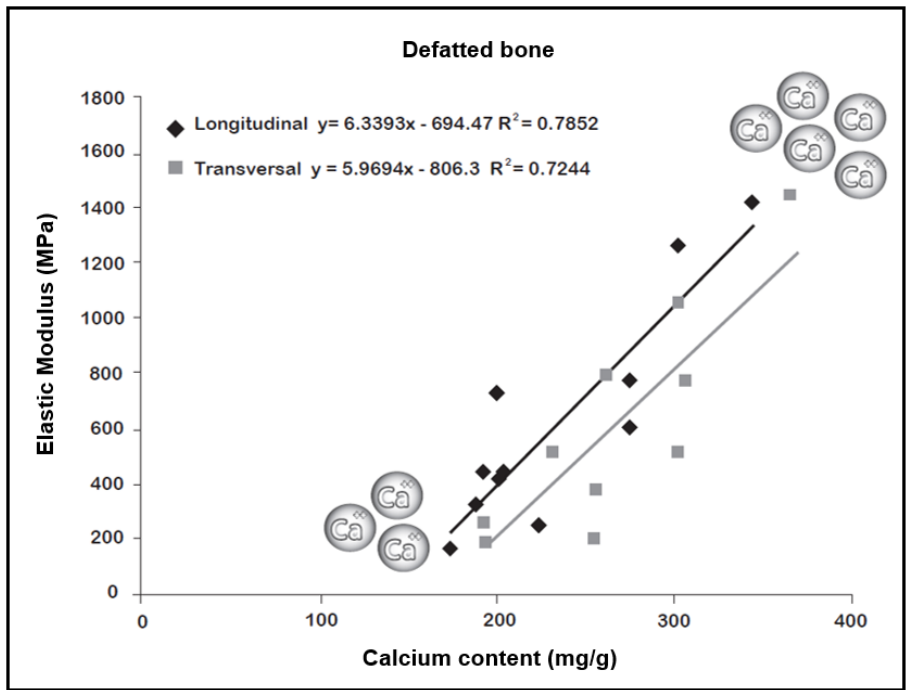
Fig. 4 (b)
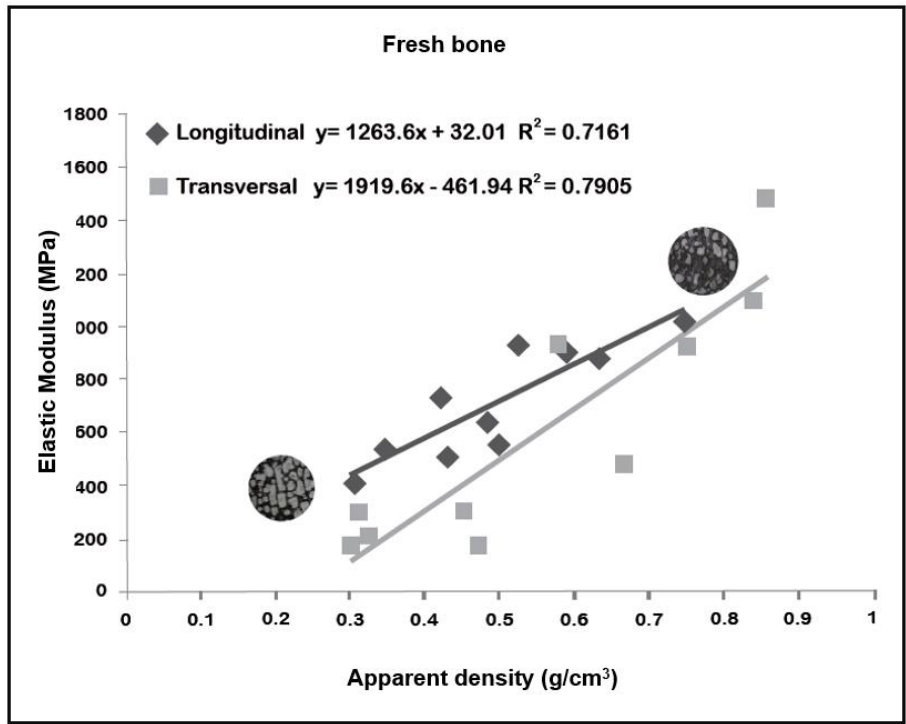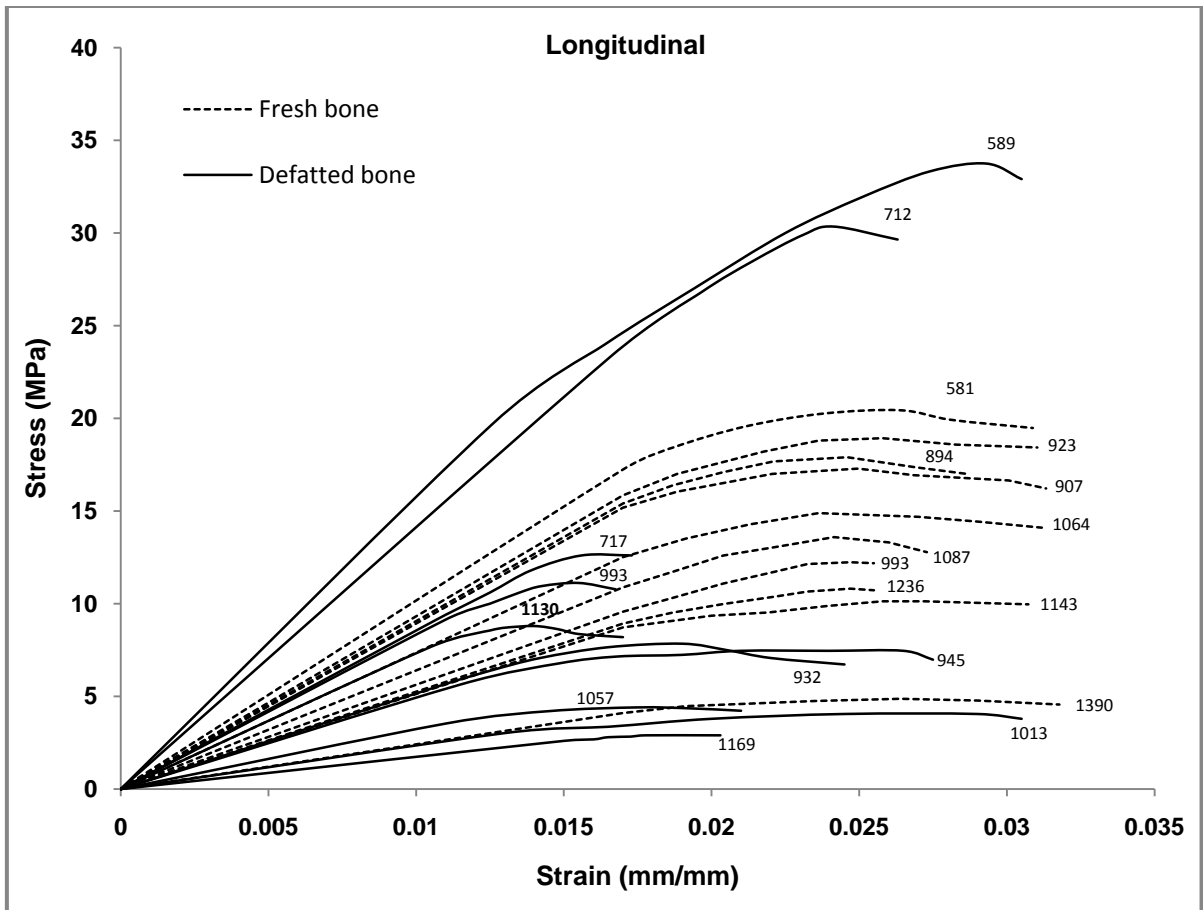
Fig. 5 (a)
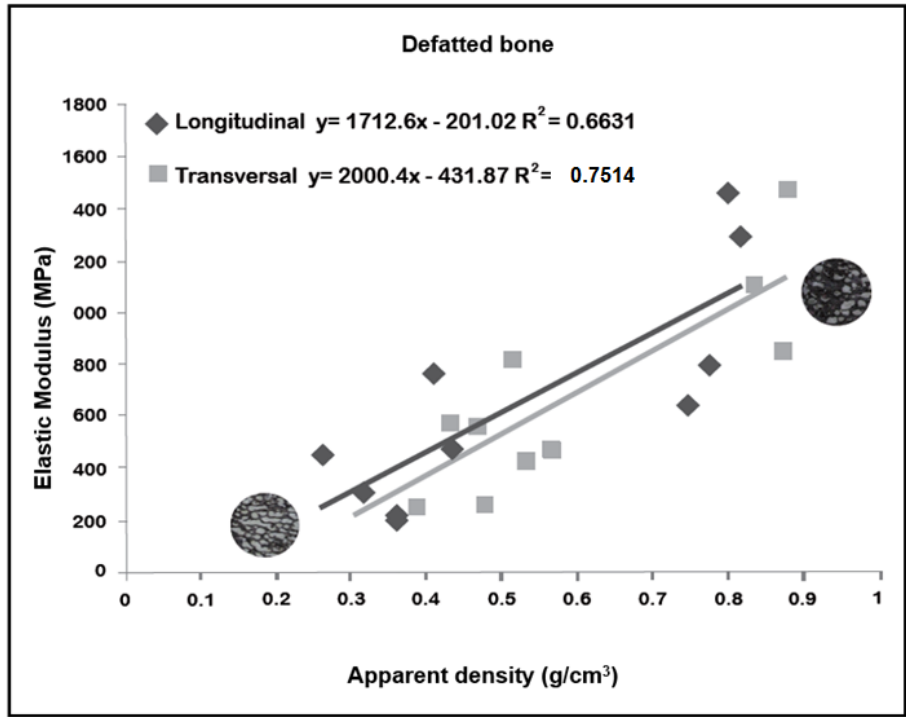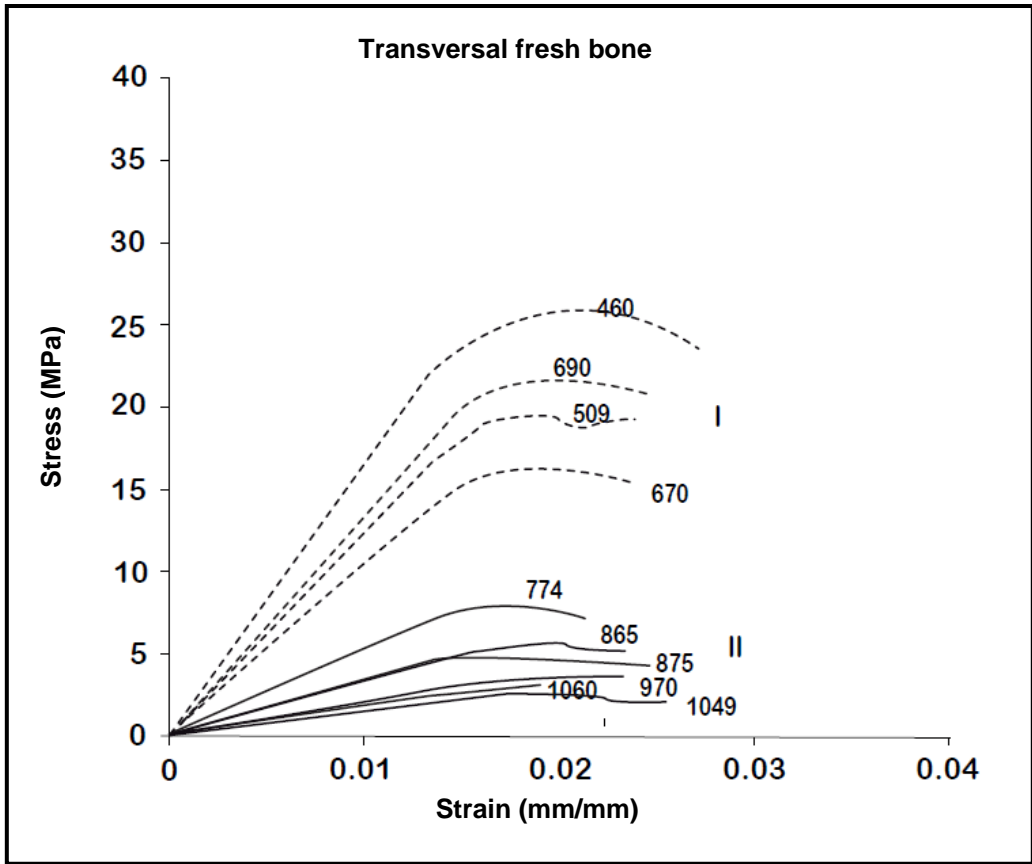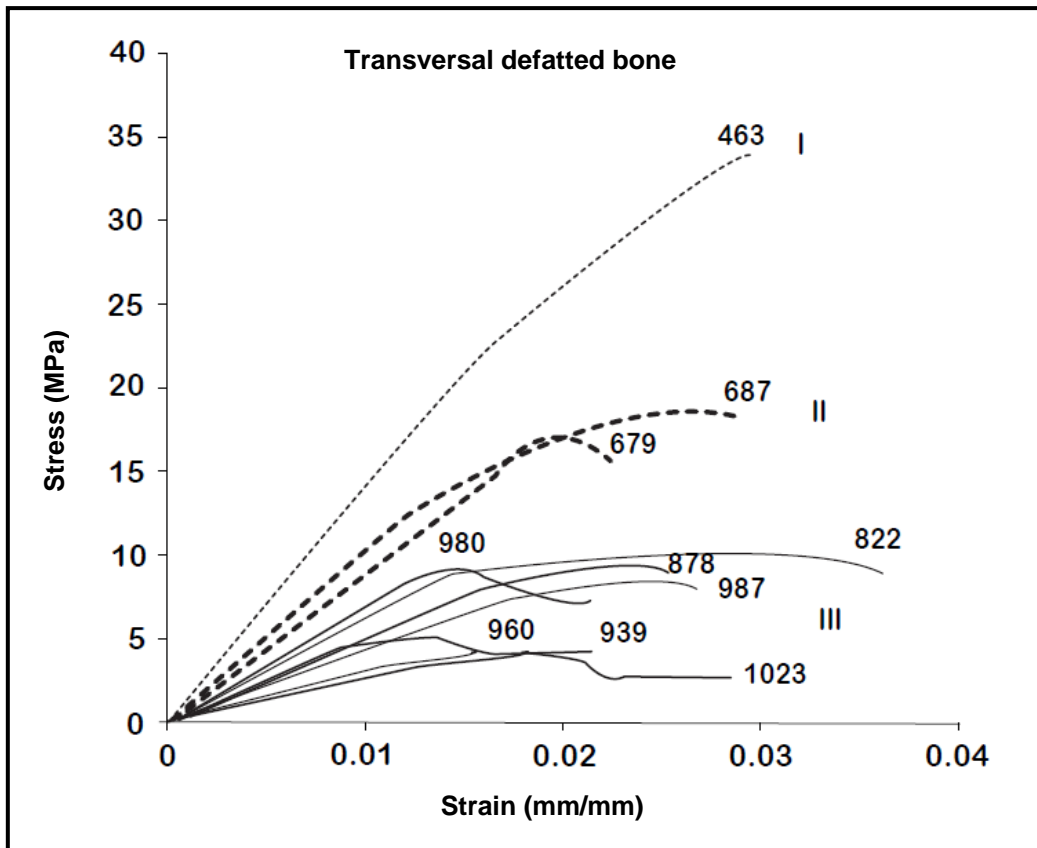

Fig. 5 (b)

Fig. 6 (a)

Fig. 6 (b)

Fig. 6 (c)

Figure captions

Fig. 1. Digital photograph of bone specimens painted black, cut (a) Longitudinal and (b) Transversal to the trabeculae. The arrows indicate the direction of the cut.

Fig. 2. Elastic modulus against total pore cross-section area. (a). Fresh bone. (b) Defatted bone.

Fig. 3. Number of pores against pore cross-section area of the four sides. Frequency polygons decay exponentially with size of pore cross-section area. The circles illustrate the porosity of the samples for high and low elastic modulus.

Fig. 4. Elastic modulus as a function of calcium content for transversal and longitudinal directions. (a) Fresh bone. (b) Defatted bone. The low Ca^+ circles represent fewer amount of calcium in bone.

Fig. 5. Elastic modulus versus apparent density showing a linear behavior for all sets of samples. (a) Fresh bone. (b) Defatted bone. The circles at the bottom are for higher porosity, the ones at the top are for lower porosity.

Fig. 6. Stress-strain curves in longitudinal orientation of the fresh and defatted bone (a). Samples cut in transversal orientation of (b) Fresh bone, (c) Defatted bone. Pore cross-section area of every sample is expressed in each stress-strain curve.

Table 1

Table 1. Amount of pores and pore cross-section area for each side and for the sum of the four sides of a transversal sample. Pore cross-section area is x , and the number of pores is y.

	Amount of pores	Pore cross-section area (mm^2)	
Side 1	462	284	y = 89.504e-0.1895x R^2 = 0.886
Side 2	435	199	y = 133.24e-0.2809x R^2 = 0.9199
Side 3	542	212	y = 156.46e-0.3092x R^2 = 0.850
Side 4	451	146	y = 153.65e-0.3507x R^2 = 0.8976
Four sides	1890	841	y = 370.1e-2.3135x R^2 = 0.9363

Table 2

Table 2. Selected exponential equations fitting the data of number of pores(y) with pore cross-section area(x), for fresh and defatted bone. Number 1 is for the sample with lower elastic modulus and number 2 for the sample with higher elastic modulus.

Orientation of the Trabeculae		Equation	Correlation Factor (R^2)	Elastic Modulus (MPa)
Fresh Bone				
Longitudinal	1	y = 839.63e-1.252x	R^2 = 0.910	410
	2	y = 1843.5e-3.952x	R^2 = 0.957	1015
Transversal	1	y = 774.87e-1.58x	R^2 = 0.904	176
	2	y = 580e-1.65x	R^2 = 0.902	1480
Defatted bone				
Longitudinal	1	y = 1411e-1.47x	R^2 = 0.987	206
	2	y = 906.05e-2.699x	R^2 = 0.977	1402
Transversal	1	y = 1100e-1.049x	R^2 = 0.988	256
	2	y = 1569e-3.804x	R^2 = 0.96	1600

Table 3

Table 3. Young modulus of human bone compared with bovine bone obtained in the current work to be used as an implant.

Reference	Region	Elastic Modulus (MPa)	Defatted	Orientation
[33]	Upper femoral	58-2248	No	Non specified
[27]	Mandibular Condyle	431	No	longitudinal
		127	No	Transversal
[34]	Proximal tibial epiphysis	286	Yes	Non specified
		218	No	
[35]	Calcaneus	45.7	Yes	Longitudinal
	Distal femur	73.5		
	Proximal femur	77.8		
	Vertebrae	41.9		
[36]	Vetebrae male	55.6	Yes	Longitudinal
	Vertebrae female	35.1		
Current work	Femoral Condyle (Bovine)	714	No	Longitudinal
		754	Yes	
		607	No	Transversal
		747	Yes	